

EVALUATION OF PASSIVE COOLING THROUGH NATURAL VENTILATION STRATEGIES IN HISTORIC RESIDENTIAL BUILDINGS USING CFD SIMULATIONS

Layla Iskandar^a, Ezgi Bay-Sahin^{b, c}, Antonio Martinez-Molina^{d, e*}, Saadet Beeson^a

^aSchool of Architecture and Planning, Klesse College of Engineering and Integrated Design, The University of Texas at San Antonio UTSA, 501 W. César E. Chávez Blvd, San Antonio, TX 78207, USA.

^bLancaster School of Architecture, Lancaster University, The LICA Building, Lancaster, LA1 4YW, UK.

^cDepartment of Architecture, Faculty of Architecture, Design and Fine Arts, Osmaniye Korkut Ata University, Karacaoglan Yerleskesi, Osmaniye, 80000, Türkiye

^dDepartment of Architecture, Design & Urbanism, Antoinette Westphal College of Media Arts and Design, Drexel University, 3501 Market St., Philadelphia, PA 19104, USA

^eDepartment of Civil, Environmental, and Architectural Engineering, College of Engineering, Drexel University, 3100 Market St, Philadelphia, PA 19104, USA

*Corresponding Author

Abstract:

Natural ventilation in hot climates has the potential to save energy by reducing the need to use mechanical systems. Particularly in historic buildings, it should be considered as a passive retrofit strategy before the addition of any mechanical systems to accommodate their unique indoor environmental characteristics and ensure their preservation. This study investigates the efficiency of multiple natural ventilation strategies in cooling a historic residential structure located in San Antonio, Texas, USA, a hot and humid climate area. It also analyzes their potential to provide a thermally comfortable indoor environment during the spring and summer. Onsite data and ASHRAE standards were used to create and validate Computational Fluid Dynamics (CFD) and energy models. Six different natural ventilation approaches were simulated, and the results were analyzed and compared. The analysis revealed that all the considered scenarios can contribute to energy savings in both seasons, especially in spring, with cross ventilation being the most efficient strategy. It also proved that the size of the openings has an impact on thermal comfort. This study demonstrated that historic preservation and thermal comfort goals can be achieved simultaneously, and the results can be replicated in multiple historic structures in similar climate regions around the globe.

Keywords: Historic Building; Computational Fluid Dynamics; Building Preservation; Natural Ventilation; Energy Simulation; Thermal Comfort.

1. Introduction

1.1. Background

In the last decade, many researchers have shown increasing attention to Indoor Environmental Quality (IEQ) in heritage buildings [1]. This topic is, without a doubt, an essential area of research when retrofitting historic structures to modern thermal comfort and energy consumption requirements. While these necessary performance improvements in historic buildings have become a recurrent strategy when working on in-use heritage buildings, preserving their inherent historical value could be challenging and multifaceted. Historic preservation requirements often impose limitations on what are considered acceptable interventions from a technological and architectural standpoint. Therefore, passive retrofit strategies should be considered before the implementation of any active systems when trying to improve the energy efficiency of heritage buildings. These structures in fact often contribute to indoor environmental stability by means of their construction materials and methods [2,3]. Additionally, the building characteristics including the shape, size, envelope, and openings size play a significant role in their hygrothermal performance [2–4]. Particularly in hot and humid climates, natural ventilation, shading devices, and other strategies, are used for passive cooling purposes [5]. Historic preservation guidelines worldwide in the last decade have stressed on the importance of considering alternative cooling techniques including natural ventilation to ensure indoor thermal comfort without compromising valuable historic materials, features and values. While mechanical cooling and mixed-mode ventilation are well researched topics, literature has revealed a gap regarding naturally ventilated residential heritage structures, especially in hot and humid climates.

1.2. Literature review

Historically, natural ventilation was one of the main means of providing thermal comfort in warm climates in the absence of mechanical cooling systems [6]. The benefits of this passive strategy extend to modern day retrofits of historic structures where natural ventilation can save energy by reducing the need to use mechanical systems [7]. Bay et al. [8] assessed the appropriateness of employing natural ventilation in a UNESCO World Heritage Site in South America characterized by high thermal mass. The findings indicate that the operation of mechanical systems can be reduced, especially during spring, where the suggested night ventilation strategy effectively maintains air temperatures and relative humidity levels within an optimal range for occupant comfort and building preservation. Laurini et al. [9] explored the potential of stack ventilation in improving hygrometric indoor comfort in a high architectural value historic building dating from the fifteenth century. The results proved that stack ventilation decreased temperature and relative humidity values and enhanced the comfort conditions especially during the summer months. Moreover, Darmanis et al. [10] emphasized the significance of integrating mixed-mode cooling systems, comprising both passive and mechanical cooling systems, within buildings as a measure to decrease the overall carbon footprint of such structures.

Regarding cooling and ventilating heritage buildings, many structures worldwide do not have mechanical systems installed, and the addition of these systems is often the primary consideration of energy retrofit projects. Since historic buildings were usually not conceived or built with any cooling or heating system in mind, installing mechanical systems such as heating, cooling, or ventilation as part of a retrofit plan is highly complicated to integrate correctly without negatively affecting the buildings' conservation of cultural values and cherished features [7]. Furthermore, this type of equipment could also decrease the efficacy of any conservation strategy for any potential artwork held in the building or the building itself [11–20]. This adverse situation and the harshness of climate zones 1A, 2A, 2B, 3A, and 3B make it

challenging to keep indoor air temperatures and relative humidity levels within thermal comfort ranges for occupants [21]. Due to a small initial economic investment and a short response time to cool and heat sizeable indoor air volumes, forced air and hot water radiators are the most frequently considered systems in historic buildings. These two mechanical approaches adapt best to historic buildings' requirements since they can be used intermittently, aiming for occupant satisfaction with the indoor thermal conditions for a short period of time or continuously maintaining constant hygrothermal conditions [22,23]. In the southern area of the United States of America (USA), heating, ventilation, and air conditioning (HVAC) systems were installed in historic buildings in the 1980s and 1990s when there were no particular regulations for installing air-conditioning in such structures. Cooling systems were designed and mounted with the unique objective of occupant comfort, categorically disregarding the preservation of the historic building. Nonetheless, it is critical to explore alternative cooling strategies, such as natural ventilation to uphold indoor thermal comfort without jeopardizing the integrity of historic materials and features.

The most important fundamental requisite in the overall ventilation process is airflow. While natural ventilation contributes to improved indoor thermal conditions, effectiveness of using wind-driven flow is a challenging task requiring multiple aspects. For example, a research study performed in residential buildings in southeast Asia suffering from a hot and humid climate revealed that natural ventilation, mainly indoor air velocity as low as 0.04m/s, is sufficient to increase occupants' thermal comfort [24]. Moreover, natural ventilation was proven to reduce the cooling load of buildings in this same climate area [25].

However, controlling natural ventilation is a nonlinear and complex problem associated with multi-dimensional parameters, and active systems are usually required to meet cooling demands, besides natural ventilation, to ensure thermal comfort and even acceptable preservation conditions [26]. These very challenging locations experience high temperatures and sometimes extreme relative humidity levels, even at

night, making natural ventilation solutions rather unsuccessful as a sole solution for cooling. At the same time, it is valuable to take advantage of natural ventilation as a passive cooling strategy to enhance energy performance. More importantly, preserving the exploitation of natural ventilation in historic buildings can prevent moisture build-up and damage to significant historic materials [27,28]. Therefore, the only option to significantly decrease the usage of mechanical cooling systems in these areas is a methodical and thorough assessment of the structure's natural ventilation potential, optimizing airflow performance. Reducing the cooling systems' run time resolves the above-mentioned possible conservation complications caused by the forced indoor conditions generated and thus should be considered as part of heritage buildings' retrofit plans.

Computational Fluid Dynamics (CFD) simulations have recently been used to investigate and improve indoor hygrothermal factors impacted by natural ventilation in heritage buildings [8,29]. It is critical that the modeler working with CFD models is knowledgeable and skilled and demonstrates sensitivity while creating the model, particularly in historic structures due to their peculiarities [30], to utilize these CFD models and achieve trustworthy results precisely. Researchers have published numerous scientific studies on developing CFD simulations in historic buildings. For example, a research endeavor in Italy applied CFD simulations in an 18th-century heritage building to optimize the performance of natural ventilation and airflow [19]. These simulations projected indoor environmental conditions and discovered that the proposed mechanical system upgrade would allow the building to gather large exhibitions with acceptable thermal comfort and historic preservation standards. A different Italian investigation used a calibrated CFD model with onsite data to simulate the energy load of the projected HVAC system replacement, recommending a heating system retrofit in a historic palace. These results and reliable outcomes of this investigation prove the compatibility of the system-historic building and establish the

indoor environment unaffected by the system modernization [31]. Abuku et al. [32] led a more comprehensive study investigating the influence of wind-driven rain on building conservation considerations (hygrothermal performance, energy usage, mold growth on interior wall surfaces, and indoor environment) utilizing CFD model simulations. By creating a CFD model, Balocco [33] applied an even more holistic approach to examining the connection between the outdoor and indoor environments with occupancy, mechanical systems, and lighting. The same researcher used another CFD model to investigate the cooling potential of an HVAC system airflow in a historic building in Palermo, Italy [34]. Since airflow is driven by pressure and temperature differentials through wall openings, structures using natural ventilation have a significant handicap due to the necessity of having a comprehensive knowledge of complex airflow patterns related to airstreams and buoyancy [35]. The capability to suggest and forecast the outdoor and mostly indoor airflow performance of diverse natural ventilation strategies is one of the main benefits of CFD models. This simulation method can evaluate several potential ventilation approaches without the necessity of obtaining field-monitored data [36] and assess the airflow in spaces with specific conservation requisites [37].

1.3. Objectives of the study

This paper explores the relationship between natural ventilation and outdoor and indoor environmental conditions in residential heritage buildings for the purpose of passive cooling under the adverse environmental circumstances of ASHRAE climate zone 2A. A validated steady-state numerical model has been used to present the outcomes of computational fluid dynamics CFD and energy simulations performed on an early listed 1900s residential building in San Antonio, Texas, USA. The particularity of this case study being located in a hot and humid climate and representing one of the most common historic residential buildings typologies in the United States has a major impact on investigating the enhancement of its indoor environmental conditions

passively. Since cooling and dehumidifying are the main concerns in such climate areas, this study focuses on validating the connection between indoor microclimate and different natural ventilation strategies during the cooling season. Furthermore, the article intends to step forward in the essential disciplinary discussion concerning the balance between occupant thermal comfort and historic preservation requirements by encouraging mixed-mode ventilation and passive cooling in lieu of exclusive mechanical cooling and ventilation.

2. Materials and Methods

To evaluate the efficiency of passive cooling through natural ventilation in historic residential buildings in a hot and humid climate, methods of field measurements and CFD building simulations are combined, as shown in Figure 1. The functions of the involved methods are elucidated as follows:

- An environmental monitoring campaign was conducted to collect indoor and outdoor environmental parameters, namely air temperature and relative humidity, to extract the elementary principles of natural ventilation and serve as baselines for the calibration of building simulations. Wind speed data was also retrieved from the San Antonio International Airport database.
- Building simulations were performed using IES VE software, consisting of integrated analysis modules such as Modelit, Suncast, Apache MacroFlo, and MicroFlo. IES VE is a reliable and trustworthy simulation tool as it enables integration between applications while providing realistic and fast results on building performance.
- [8,38–45]The model was calibrated using the measured data from the on-site monitoring. Several models were created to evaluate different natural ventilation scenarios that were proposed by the building management and the research team based on several factors such as feasibility, cooling potential and cultural

preservation. These analyzed scenarios are: 1- no natural ventilation; 2A- ventilation with openings at full capacity; 2B- ventilation with openings at half capacity; 3- cross ventilation; 4- stack ventilation; 5- night flush ventilation.

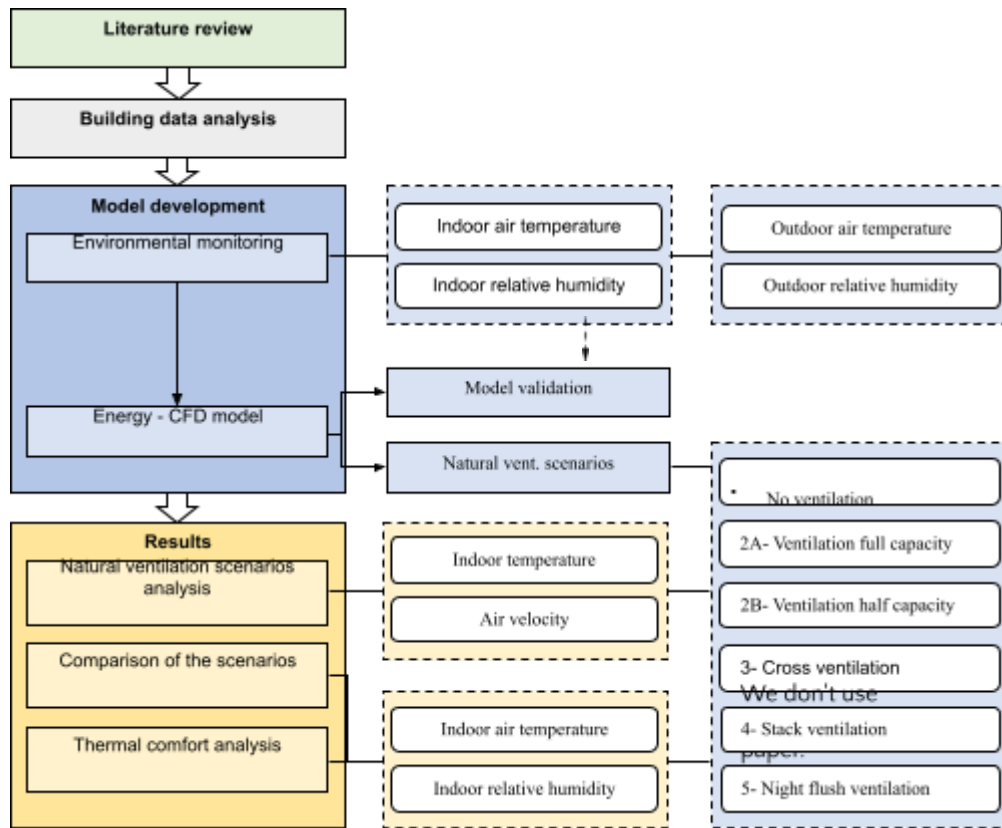


Figure 1. Flowchart of the adopted methodology.

2.1. Building description

The case study is the Kelso house in San Antonio, Texas. Located at 240.5 meters (m) above sea level, San Antonio has a Cfa-Humid Subtropical Climate with a Bsk-Semi-Arid Climate on its west part according to the Köppen-Geiger climate classification [38]. Over the year, the temperature varies from 9.00°C on average during the coldest months to 32.00°C during the hottest months, with 21.00°C as the annual average temperature over the last 20 years. Additionally, summer temperatures reach a high of 38.00°C [39].

Famous architect Atlee B. Ayres designed the building in 1907 for the eminent judge and civic leader Winchester Kelso [40]. Featuring a simplified Neoclassical style

with Queen Anne and Craftsman influences [41], the structure is designated on the National Register of Historic Places as a contributing property to the Monte Vista National Historic District located north of Downtown. The wood-frame structure is 11 meters high and has an irregular and asymmetrical plan arrangement and complex roof proportions reflecting the craftsman influence. The facades are asymmetrical, finished with painted wood teardrop siding and shingles with trim. The building features a two-story porch wrapping around the south and east, wood-frame windows, and neoclassical decorative elements, including grandiose Doric columns, wood-trimmed entablature with frieze, dentils, cornice, and wood balustrades. The characteristics of the building components are summarized in Table 1.

A local foundation named The Power of Preservation Foundation (PoP) acquired the property in 2018 and restored the building's exterior (Figure 2). The interior remains in poor condition and the building unoccupied, but the foundation plans to rehabilitate it and restore its functionality. Planning entails a holistic approach that considers enhancing the house's energy performance and meeting the needs of adaptive reuse without altering cherished historic materials and features.



Figure 2. The Kelso House view from the south-east side before the exterior restoration (left). Source: (Power of Preservation Foundation 2022) and after the restoration (right). Source: (Biediger 2021).

Table 1. Characteristics of the building components.

Building components	Material	Thickness(mm)	Resistance(m ² K/W)	Density(kg/m ³)
Walls	Wood	127	0.46	560
Partitions	Wood	127	0.47	500
Roof	Wood	128	0.91	530

Ground floor	Wood	38	0.31	649
Windows	Single pane – Wood frame	3	0.15	-

2.2. Environmental monitoring

A network of 13 indoor and two outdoor data loggers was purposefully positioned in the building, as displayed in Figure 3, to evaluate the existing environmental conditions. These devices monitored indoor and outdoor temperature (°C) and relative humidity (%) conditions from May to September 2022 during the cooling season. The positioning adhered to the requirements of ASHRAE 55 [42], which stipulate a distance of 1.0 m inward from the room's wall and the center of the largest window, as well as 1.1 m above the floor. This height simplifies the spatial average calculation, considering 1.1 m as a common approximation to the numerical average of acquiring environmental conditions for seated (0.1, 0.6, and 1.1 m) and standing occupants (0.1, 1.1, and 1.7 m). This approximation was necessary due to limitations on the available monitoring devices for this investigation, and to avert imprecise measurements. Table 2 details the characteristics of the monitoring devices.

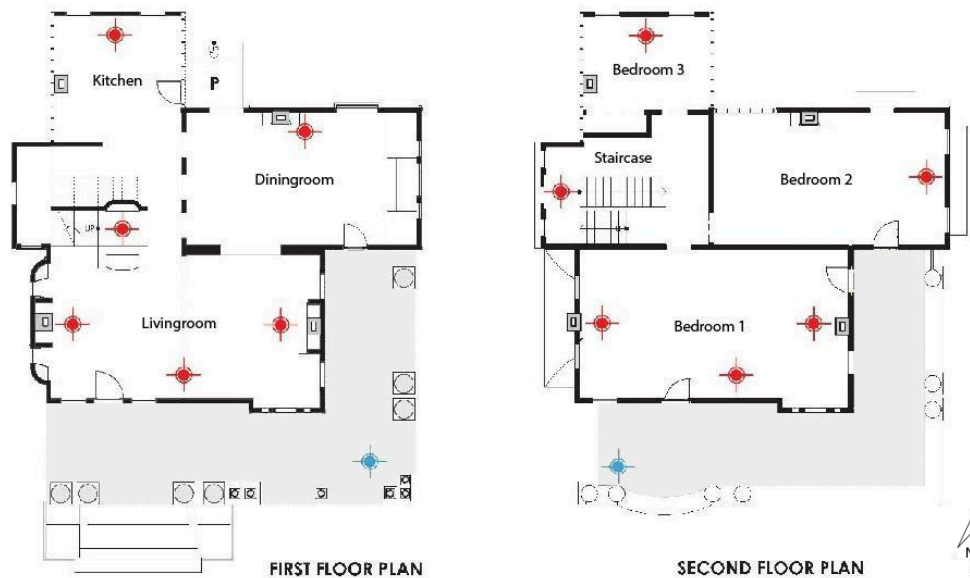


Figure 3. Locations of the indoor (red) and outdoor (blue) temperature and relative humidity data loggers on the first level (left) and second level (right). An additional data logger is positioned on the attic level.

Table 2. Specifications of the data loggers

Measured Physical Variables	Brand and Model	Measuring Range	Precision	Response Time
Indoor Air Temperature	HOBO® MX1101	-20.00° to 70.00°C	±0.21°C	60 seconds
Indoor Relative Humidity	HOBO® MX1101	1% to 90%	±2.0%	20 seconds
Outdoor Air Temperature	HOBO® MX 2301A	-40.00 to 70.00°C	±0.25°C	60 seconds
Outdoor Relative Humidity	HOBO® MX 2301A	0 to 100%	±2.5%	30 seconds

Physical variables were set to be recorded every 15 minutes to acquire a wide range of the environmental conditions inside the building. This frequency additionally provided the necessary information to identify any reoccurring patterns or radical deviations throughout the study. Figure 4 displays the monitored minimum, maximum, and average indoor and outdoor temperatures, and average indoor and outdoor relative humidity conditions.

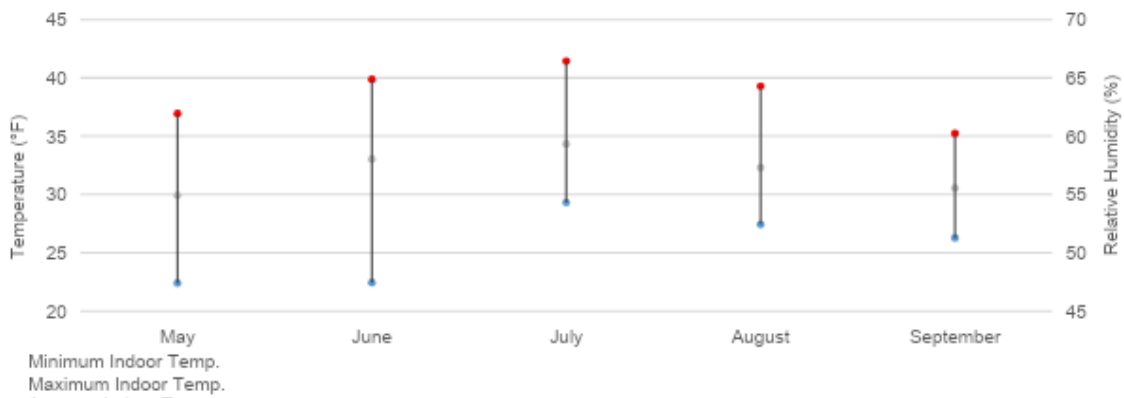


Figure 4. Indoor and outdoor environmental conditions monitored by the data loggers during the period of study.

Moreover, the wind speed data, one of the most important variables impacting natural ventilation, was retrieved from the San Antonio Airport (SAT) weather station for the study period. The data is presented in Figure 5.

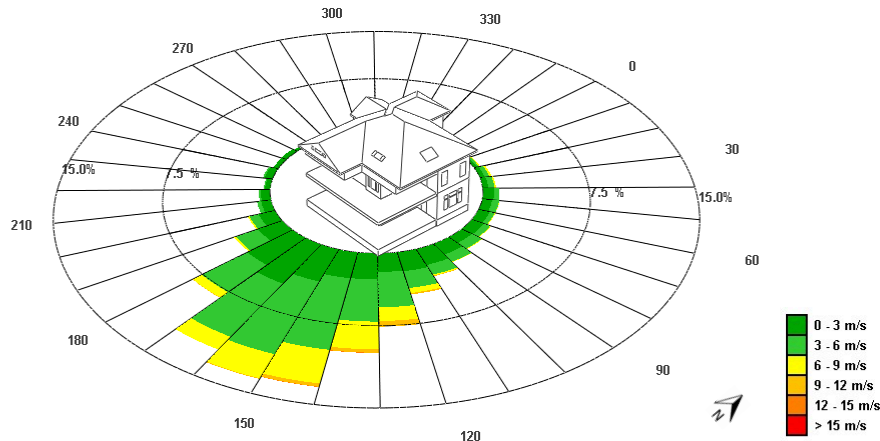


Figure 5. A wind rose illustrating the airflow (m/s) during the study period spanning from May to September.

2.3. Natural ventilation scenarios

Five scenarios were analyzed in free-floating conditions, without the use of HVAC, to assess the passive cooling opportunities in the studied building. These scenarios were chosen considering the recommendations of the building management, drawing on decades of experience in employing natural ventilation methods commonly used in this geographical region for historic buildings. Additionally, local preservation organizations supported these strategies, deeming them feasible and responsible for cultural and heritage preservation. The different scenarios examine the impact of natural ventilation through the windows, cross ventilation for prevailing winds, stack ventilation, and night flush.

- Scenario 1: The studied building is investigated without any natural ventilation occurring; only air infiltration is considered. This scenario is intended to be used as a reference for comparison purposes. The windows are fully closed at all times.
- Scenario 2: All windows are open to allow natural ventilation, in addition to the consideration of air infiltration. In this case, two sub-scenarios were examined:
 - Scenario 2A: All windows are always open to full capacity.

- Scenario 2B: All windows are always open to half capacity.
- Scenario 3: All windows on the south and north facades are open on the first and second floors to always allow cross ventilation for prevailing winds. The attic access door and windows are closed at all times.
- Scenario 4: This scenario examines the stack ventilation effect. All windows on the first floor and the attic access door and windows are open, while the windows located on the second floor are always closed.
- Scenario 5: All windows on the first and second floors are open between 21:00 and 6:00 to allow for night ventilation. During these times, the attic access door and windows are closed.

Energy and CFD simulations were run to evaluate the efficiency of each scenario. Two representative days in the cooling period were chosen to run the simulation: May 8 to examine cooling in the spring and July 23 to analyze cooling in the summer (Figure 4).

2.4. Energy and computational fluid dynamics (CFD) model

Building energy modeling is a widely accepted method for design evaluation and assessment of operation systems. Particularly for natural ventilation studies, Computational Fluid Dynamics (CFD) is commonly used to understand how the air travels around the objects in building areas and outside buildings [43]. This study used the IES VE software, used in many scientific publications [8,38–45], to perform energy and CFD simulations [44]. Incorporating location and real weather data, the 3D model geometry of the case study can be generated with or without BIM integration. HVAC design, solar, and wind study applications are also available. Especially for natural ventilation studies, IES VE MicroFlo provides quick results since it is easy to set up and run. Compared to other methods such as wind tunnel tests and experimental studies, design time and costs are usually lower. Including various modules, the software uses

the Apache Simulation results to automatically set up boundary conditions for the CFD model. This module is a core application of the software performing advanced dynamic thermal simulation at time steps across a whole year or over selected days. Multiple parameters such as velocity components, pressure, and temperature are available throughout the domain. With another module, MacroFlo, airflow driven by wind pressure and buoyancy forces can be simulated to analyze the feasibility of various strategies. The software also provides thermal comfort parameter results. Although curved geometry may cause some problems adding complexity to the grid, our model geometry was set to align the axes since the case study was a rectangular building without any curves. Providing a large library of constructions and materials, renewable energy sources, schedule systems, and equipment, the inputs can be edited.

This building simulation tool was used to create the case study's energy model and determine the boundary conditions that were later used for the CFD model. Boundary conditions include data such as surface temperatures, heat gains and losses, and airflow rates through the building openings. The CFD model investigated heat transfer processes, airflow trends, buoyancy, and wind-driven ventilation indoors and outdoors. The analysis was based on the 'Finite Volume Method' [45]

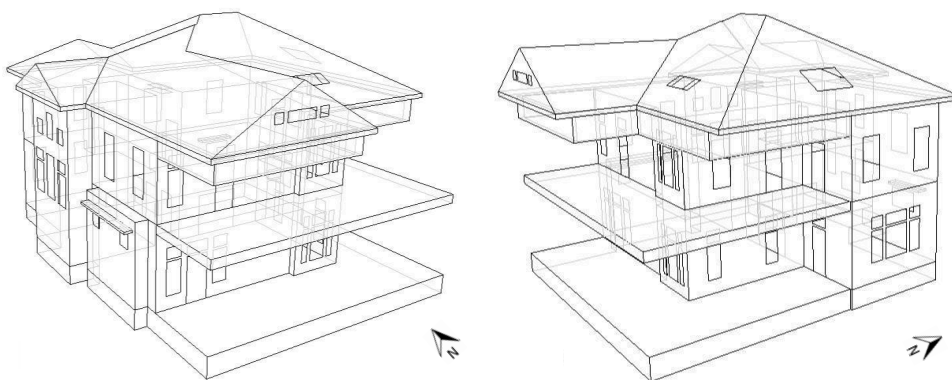


Figure 6. The simplified model of the building in the IES VE software.

A series of established simulation steps were utilized to create the energy and CFD models. First, the input data, including the building parameters and weather data, were

defined in the ModelIt module within IES VE and the building model (Figure 6). Since the impact of input data accuracy on the analysis results is critical to create realistic assumptions and match the real-world conditions, the building and site properties (geometry, orientation, window-to-wall ratio, construction material, glazing, interior walls, flooring, etc.) were meticulously collected and modeled. The specifications of the CFD model used in IES VE ModelIt and Microflo are summarized in Table 3.

Table 3. Model dimensions and specifications of the CFD model used in IES VE ModelIt and MicroFlo.

Floor surface area (m ²)	703.1400	Number of cells (million)	3.2-3.4
Volume (m ³)	1369.9207	Max cell aspect ratio	<12:1
Ext wall area (m ²)	456.3263	Turbulence model	k-e
Ext opening area (m ²)	61.8600	Grid line merge tolerance (m)	0.01

Climatic variables play an essential role in assessing natural ventilation in buildings. Therefore, using a proper and comprehensive weather file of the appropriate location settings is highly significant. A Typical Meteorological Year (TMY3) file was used as the required input for the energy simulation. The weather file includes variables such as dry bulb temperature, wet bulb temperature, solar altitude and azimuth, cloud cover, wind speed, and direction gathered from the San Antonio Airport (SAT) weather station.

As the building is unoccupied, the monitored data was collected while the structure was vacant, and the model run was performed without any occupancy variations to obtain accurate simulation results. Apache module was used to modify time-varying window openings in Scenario 5. Repeating daily profiles for night ventilation were organized, and this pattern was applied over a year via an annual profile. Based on this, during the spring and summer seasons, natural ventilation only occurs between 21:00 and 6:00.

Various studies have also used the IES VE MicroFlo module to run Computational Fluid Dynamic (CFD) simulations. In this study, only internal CFD simulations were used. As the first step, boundary conditions from the energy model results in VistaPro

were exported to MicroFlo, enabling users to determine wind outcomes in the building during the spring and summer seasons for cooling and ventilation purposes. Exported data on boundary conditions included the prevailing wind direction, wind speed, and indoor and outdoor air temperatures. Table 4 displays the specifications of the CFD model.

Table 4. Model dimensions and Specifications of the CFD model.

IES VE Modellt		IES VE MicroFlo	
Floor surface area (m ²)	703.1400	Number of cells	3276350
Volume (m ³)	1369.9207	Max cell aspect ratio	<12:1
Ext wall area (m ²)	456.3263	Turbulence model	k-e
Ext opening area (m ²)	61.8600	Grid line merge tolerance (m)	0.01

MicroFlo uses the Apache Simulation results to automatically configure the boundary conditions of the specific day and time for the CFD model. For the internal CFD simulations, boundary conditions were exported from VistaPro for the representative days into MicroFlo module. The boundary conditions file includes atmospheric data such as temperature, atmospheric pressure, and external moisture content; room data such as room air temperature and room radiant temperature; and surface data such as wall/window surface temperature.

The predominant air flow direction aligns with the model grid axes. Prior to running the CFD simulations, inlets and outlets were checked to ensure they functioned as expected in MacroFlo. The outdoor air temperatures at 12 pm were 25.5°C and 28.9°C on May 8 and July 23, respectively. The external relative humidity levels were 79% on May 8, dropping to 67% on July 23. Wind speed was 6.1 m/s at midday on May 8 and 2.1 m/s on July 23. The wind direction was southwest during both times.

The CFD grid was created keeping the maximum cell aspect ratio under 12:1, which, together with the grid cell sizes, provided a high level of resolution to optimize the results' accuracy. Also, the k-e turbulence model was used in this study to calculate

each grid cell's turbulent viscosity. For the sufficient mesh density in between obstacles, more than 3 million grid cells with the 0.01 m grid line merge tolerance were used (Table 4). The CFD model provided a deeper insight and graphical output to compare the selected natural ventilation scenarios. After running multiple simulations, CFD graphs were created for each potential scenario to assess and investigate the adequate natural ventilation strategy with the higher potential for cooling the structure.

2.5. Model validation

The hourly indoor air temperature and relative humidity minimum and maximum range measurements acquired from the environmental monitoring campaign were compared to the hourly average modeled values for four representative spring and summer days to predict the accuracy levels in the created energy model, as shown in Figure 7. These variables were selected for validation since they are used to analyze the impact of the natural ventilation scenarios on environmental conditions and the thermal comfort of occupants, as well as to compare the effectiveness of these scenarios [46–49]. It is important to note that both the measured and simulated data are at the testing height of 1.10 m. Specifically, May 7 and May 8 were chosen as two consecutive days for validation in spring, with May 8 serving as the spring representative day analyzed in this study. Similarly, July 23 and July 24 were selected as two consecutive days for validation during the summer, with July 23 being the summer representative day examined in this study. The two primary uncertainty indices recommended by ASHRAE Guideline 14 [50], namely mean biased error NMBE, and the coefficient of variation of the root mean square error, CV(RMSE), were used. The NMBE and CV (RMSE) were calculated using Eq. (1) and Eq. (2), respectively.

$$Eq. (1): NMBE = \frac{1}{\bar{Y}} \frac{\sum_{i=1}^N (Y_i - \hat{Y}_i)}{N-p} \times 100$$

$$Eq. (2): CV(RMSE) = \frac{1}{\bar{Y}} \sqrt{\frac{\sum_{i=1}^N (Y_i - \hat{Y}_i)^2}{N-p}} \times 100$$

Where Y_i is the measured value, \hat{Y}_i is the simulated value, \bar{Y} is the average of measured values, N is the number of data points, and p is the adjustable model parameter. According to ASHRAE, the NMBE and CV(RMSE) limit should not surpass $\pm 10\%$ and 30%, respectively, for hourly calibration. For the case study energy model, the analysis resulted in NMBE and CV(RMSE) values of 4.32% and 5.42% for indoor temperature, and 3.87% and 13.91% for relative humidity on May 7, respectively. On May 8, the values were 5.02% and 6.23% for indoor temperature, and 4.38% and 8.5% for relative humidity, respectively. For July 23, the values were -0.28% and 3.02% for indoor temperature, and -2.33% and 5.84% for relative humidity, respectively. On July 24, the values were -2.2% and 3.19% for indoor temperature, and 2.96% and 4.42% for relative humidity, respectively, as depicted in Figure 7. The NMBE and CV (RMSE) met the requirements of the ASHRAE 14 Guideline [50], which resulted in the validation of the model predictions, considering the model reliable and accurate.

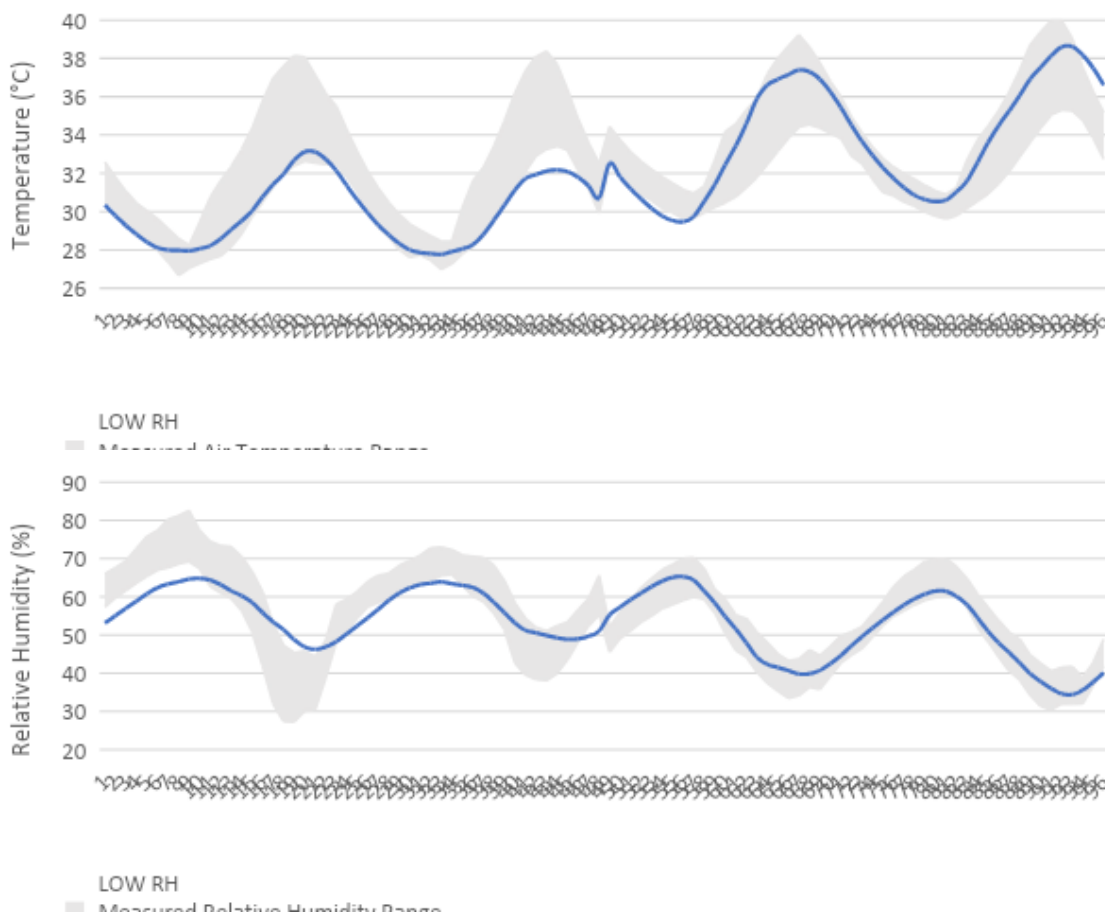


Figure 7. Comparison of hourly indoor air temperature (top) and relative humidity (bottom) measured and simulated for the Kelso House on May 8, May 9, and July 23 and July 24.

3. Results and discussion

3.1. Natural ventilation scenarios results

The CFD simulations were run for the two representative days, May 8 (spring) and July 23 (summer), to obtain air temperature, relative humidity, and air velocity values. Since the building is vacant, midday (12:00) was selected by the authors as the time to run the simulations. The five scenarios were carefully chosen to examine the significance of a specific strategy, such as the impact of ventilation with windows open, cross ventilation, stack ventilation, or night flush cooling. The building was analyzed in its free-floating state, without the presence of any occupants nor the use of any mechanical systems, to acquire a deep understanding of the inherent airflow patterns, excluding any additional influencing factors. The indoor air temperature values in the simulation ranged between 25.00°C and 29.00°C in May and between 28.00°C and 32.00°C in July. Even though average outdoor wind speeds for the selected representative days were 4.9 m/s and 1.5 m/s on May 8 and July 23, respectively, indoor air velocity values ranged between 0.00 m/s and 1.65 m/s for both studied days.

During the environmental monitoring campaign, indoor data loggers were positioned 1.1 m high above floor level, in accordance with the requirements of ASHRAE 55 [42]. For consistent comparative results, CFD graphs (both temperature and velocity) were generated at that same height. The generated temperature and air velocity graphs for all scenarios show the average values of the entire floor level at the studied time (midday) for both representative days (May 8 and July 23).

3.1.1. Scenario 1 (Benchmark): No natural ventilation

Scenario 1 analyzed the studied building without any natural ventilation to serve as a benchmark for comparison with other ventilation strategies. Figure 8 displays the air temperature distribution for May 8 and July 23. The temperature was higher on the

second floor due to thermal stratification both in spring and summer (Figure 8c and Figure 8f). Notably, the air temperature was also generally uniform throughout both floors. However, the living room on the first floor was slightly cooler (reference Figure 3 for the rooms' distribution), especially in spring (Figure 8a) due to the presence of the porch and shading devices on the south, east, and west parts of the building. Also, the temperature was the lowest at the bottom of the staircase on both representative days due to the stack effect (Figure 8a and Figure 8b). Finally, no significant air movement was noted because of the windows being closed.

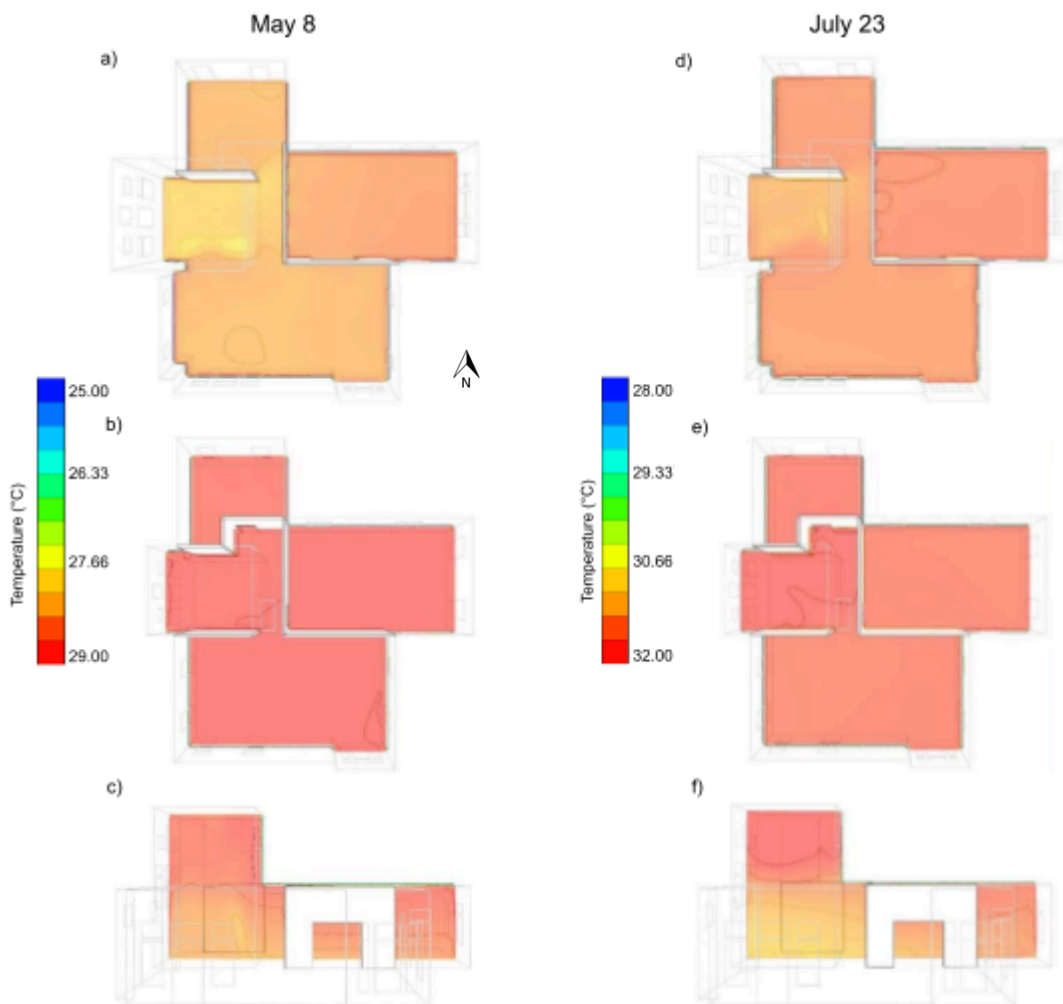


Figure 8. Air temperature graphs for scenario 1 on May 8, 2022. a) air temperature – first floor plan; b) air temperature – second floor plan; c) air temperature – vertical east-west section through the staircase. July 23, 2022. d) air temperature – first floor plan; e) air temperature – second floor plan; f) air temperature – vertical east-west section through the staircase.

3.1.2. Scenario 2: Natural ventilation with different opening sizes

In hot climates and under the necessary environmental conditions, opening windows forces outside air into the building, which prevents heat buildup and creates an effective cooling effect. This scenario aimed to evaluate the effectiveness of natural ventilation in cooling the selected case study. Historic structures in similar climate zones usually relied on large openings for better cooling outcomes through natural ventilation [7]. Two sub-scenarios were considered to investigate the consequences of having different opening sizes: Scenario 2A, which supposed that the existing windows were all fully open on the first and second floors, and Scenario 2B, where the windows were open only at half capacity.

3.1.2.1. Scenario 2A: Natural ventilation with openings operative at full capacity

Figure 9 displays the results of this scenario for air temperature and airflow. As seen in Figure 9a and Figure 9b, the air entering the building through the windows had a cooling effect since temperatures were lower by the openings. The high air velocity, reaching 1.65 m/s (Figure 9c and Figure 9d), caused an effective air movement, thus cooling the indoor spaces. Conversely, the air movement was slower on July 23, with the air velocity reaching 0.75 m/s (Figure 9g and Figure 9h), which resulted in an even distribution of the temperatures throughout spaces on the same level (Figure 9e and Figure 9f). On the spring representative day, the coolest rooms in the building were those located on the south and east due to being aligned with the prevailing winds' direction. Moreover, the living room on the first floor was the coolest space as the porch shades it, and the staircase by means of the stack effect. Both in spring and summer, the temperature on the second floor was slightly higher than on the first floor and was the highest in the attic, by around 3.00°C in spring and 2.00°C in summer, due to the increased solar radiation, which raises the radiant temperature.

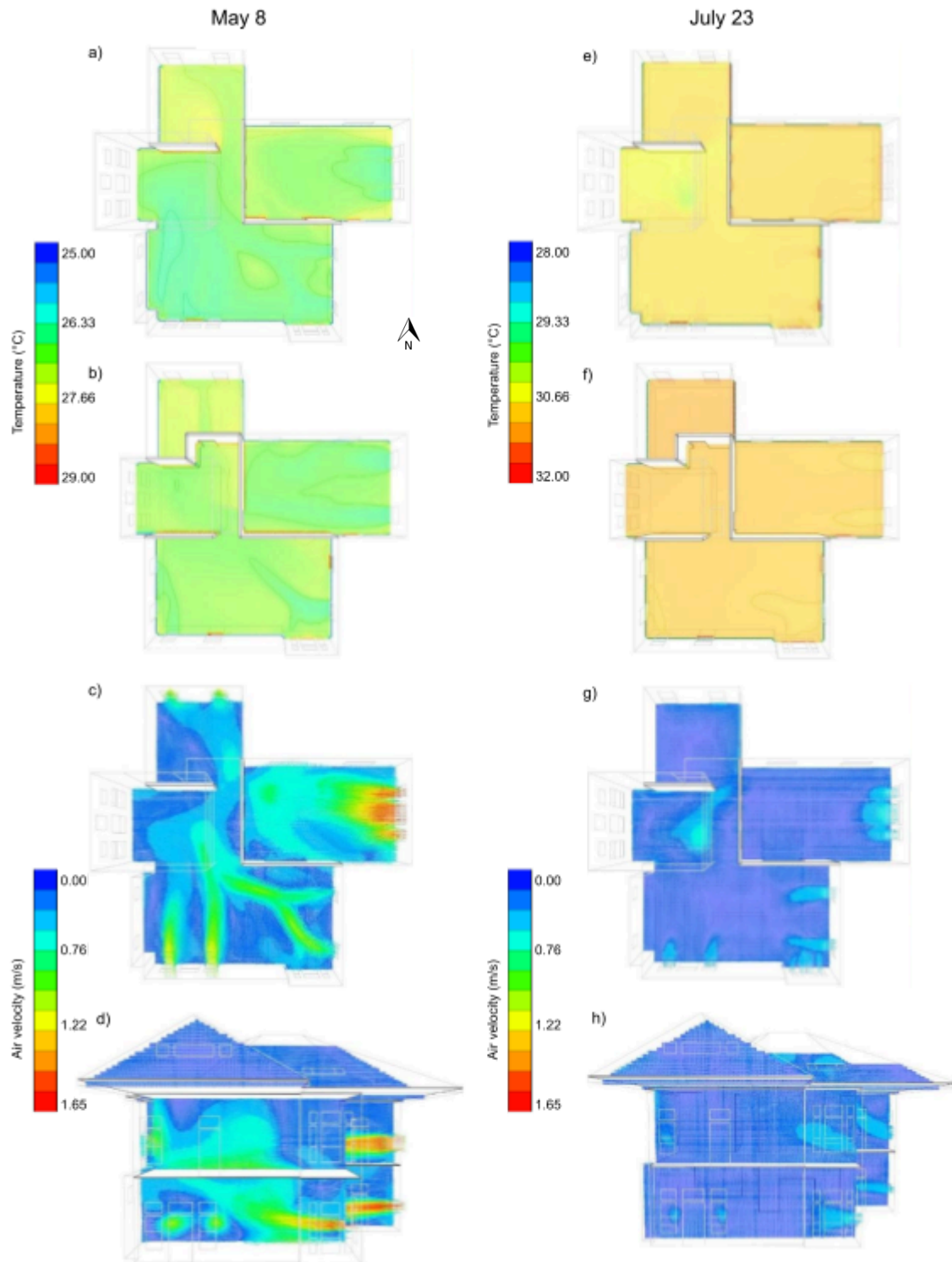


Figure 9. Air temperature and airflow graphs for scenario 2A on May 8, 2022. a) air temperature – first floor plan; b) air temperature – second floor plan; c) airflow – first floor plan; d) airflow – vertical east-west section. July 23, 2022. e) air temperature – first floor plan; f) air temperature – second floor plan; g) airflow – first floor plan; h) airflow – vertical east-west section.

3.1.2.2. Scenario 2B: Natural ventilation with openings operative at half capacity

The results for Scenario 2B showed that the air velocity was generally lower in this scenario compared to Scenario 2A, both on May 8 and July 23 (Figure 10), which the reduction in the opening sizes could explain. Exceptionally, the airflow in the living room on May 8 was higher than that in Scenario 2A because of the air channeling effect. Nevertheless, no significant impact on indoor air temperature and relative humidity was perceived, neither in spring nor summer.

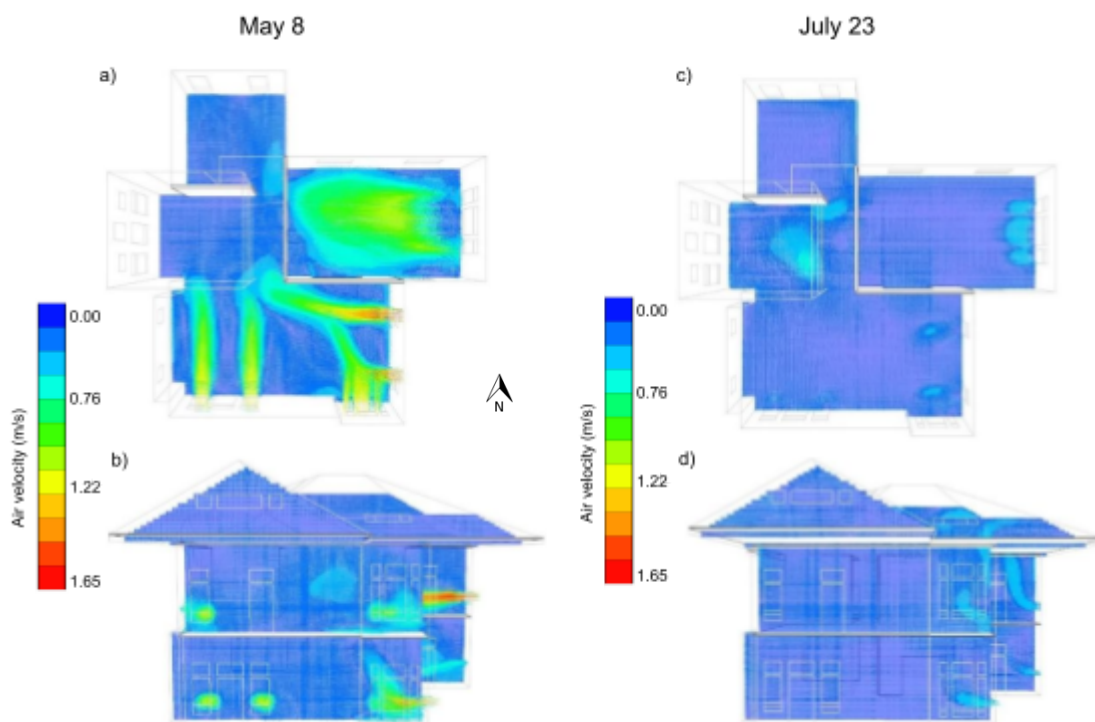


Figure 10. Airflow graphs for scenario 2B on May 8, 2022. a) airflow – first floor plan; b) airflow – vertical east-west section. July 23, 2022. c) airflow – first floor plan; d) airflow – vertical east-west section.

3.1.3. Scenario 3: Cross ventilation

Cross ventilation relies on wind-driven force to get cooler air from outside and replace the interior warm air by producing a cool stream and current across the space. Scenario 3 analyzed the impact of this strategy, where the north and south windows were considered open on the first and second floors. Figure 11 displays the results for air temperature and airflow. Figure 11a and Figure 11b show that this strategy lowered the temperature, especially in the exposed areas. The position and size of the

openings also had a significant role in the cooling effect of this strategy. The high airflow successfully contributed to creating a current throughout the space during the spring representative day, as displayed in Figure 11c. However, the low air velocity during the summer representative day (Figure 11f) prevented any variation in the temperature throughout the indoor spaces (Figure 11d and Figure 11e). Moreover, thermal stratification resulted in slightly higher temperatures on the second floor in spring and summer.

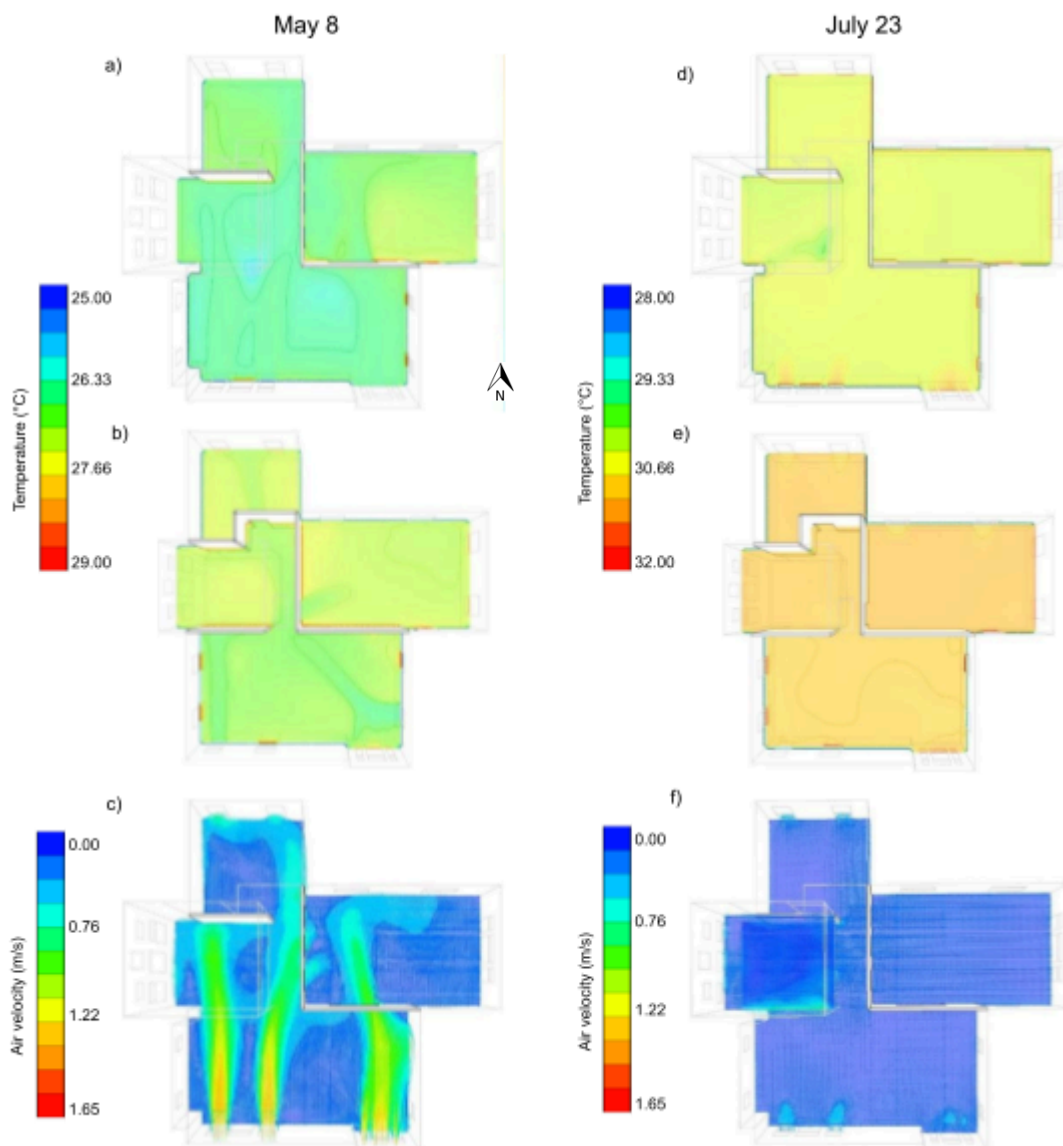


Figure 11. Air temperature and airflow graphs for scenario 3 on May 8, 2022. a) air temperature – first floor plan; b) air temperature – second floor plan; c) airflow – first floor plan; July 23, 2022. d) air temperature – first floor plan; e) air temperature – second floor plan; f) airflow – first floor plan.

3.1.4. Scenario 4: Stack ventilation

Stack ventilation relies on temperature differences to move the hot air up due to buoyancy, leaving the outside air with lower pressure inside the building. As seen in Figure 12c and Figure 12d, the air entering the building during the spring representative day flowed towards the staircase and moved up towards the attic. The temperature was lower in the exposed areas on the first floor (Figure 12a), particularly on the east and south (direction of the prevailing winds). Figure 12b shows that the staircase was the coolest area on the second floor, while temperatures were higher in the other rooms, especially in bedroom 2 (reference Figure 3 for the rooms' distribution). Even though the air movement was prolonged during the summer representative day, it was slightly faster on the staircase (Figure 12h). However, no temperature difference was perceived throughout the spaces (Figure 12e and Figure 12f).

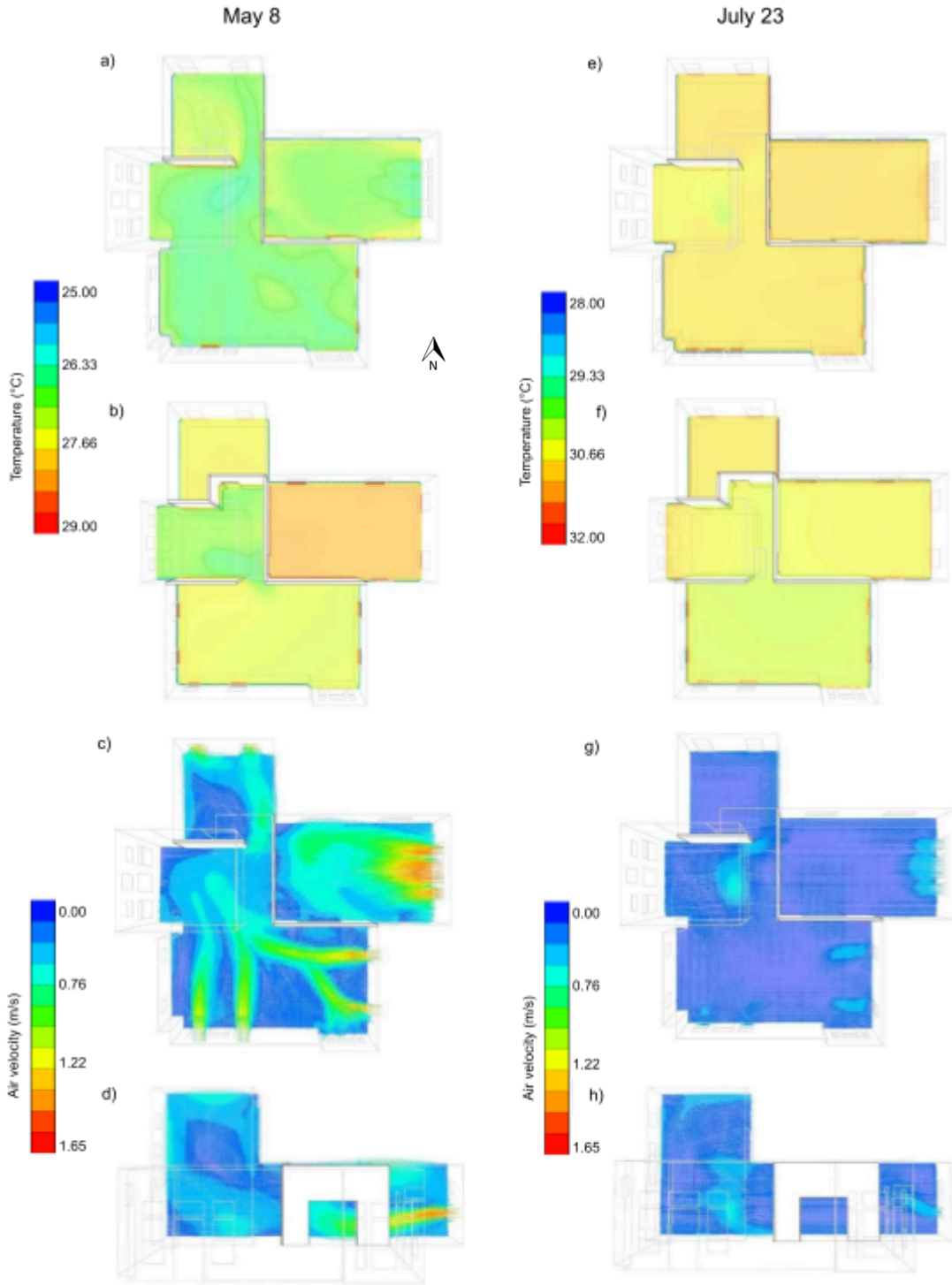


Figure 12. Air temperature and airflow graphs for scenario 4 on May 8, 2022. a) air temperature – first floor plan; b) air temperature – second floor plan; c) airflow – first floor plan; d) airflow – vertical east-west section through the staircase. July 23, 2022. e) air temperature – first floor plan; f) air temperature – second floor plan; g) airflow – first floor plan; h) airflow – vertical east-west section through the staircase.

3.1.5. Scenario 5: Night flush cooling

Night flushing allows the cooler night air to enter the building, aiming to discard heat build-up gathered throughout the day, and is considered as an indirect way to cool buildings [51]. To investigate this strategy, the authors considered that windows were open from 21:00 to 6:00 and closed at all other times. Unlike the scenarios above, simulations were executed at 21:00, 6:00, and 12:00 to understand the effect of night ventilation better. Even though these three times were considered in the analysis of the results, only the graphs at 12:00 were displayed (Figure 13) for comparison with the other scenarios.

Both in spring and summer, the air temperature decreased significantly after windows were open at 21:00 and continued to be reduced. However, once windows were closed at 6:00, the temperature started rising again, proving that cooler temperatures cannot be maintained due to night ventilation. Particularly in summer, even when outdoor temperatures reached thermally comfortable temperatures, this strategy failed to lower the indoor temperature quickly enough to create a thermally comfortable environment. On the spring representative day, the temperature was higher on the second floor, and the coolest temperature was recorded on the staircase on the first floor due to thermal stratification (Figure 13c).

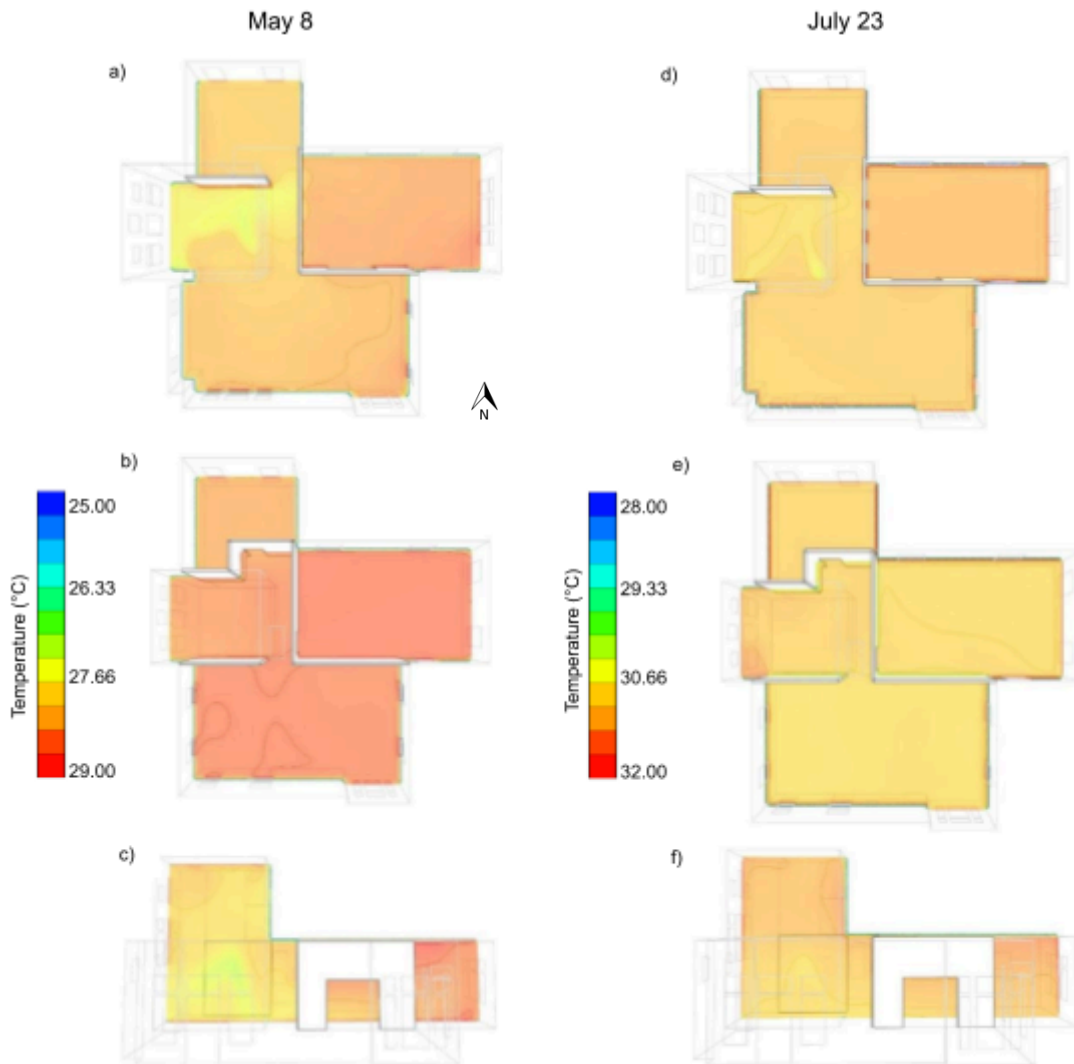


Figure 13. Air temperature graphs for scenario 5 on May 8, 2022. a) air temperature – first floor plan; b) air temperature – second floor plan; c) air temperature – vertical east-west section through the staircase. July 23, 2022. d) air temperature – first floor plan; e) air temperature – second floor plan; f) air temperature – vertical east-west section through the staircase.

3.2. Comparison of the effectiveness of different scenarios

The indoor air temperature and relative humidity values resulting from the simulations were compared among the different scenarios and to the outdoor temperature and relative humidity values during the spring (Figure 14 and Figure 15) and the summer (Figure 16 and Figure 17) representative days to identify the best natural ventilation strategy for cooling the building.

As displayed in Figure 14, the outdoor temperature on the representative spring day changed between 22.20°C and 30.00°C. It increased after 8:00 and reached the maximum value between 14:00 and 15:00, then began to decrease. The outdoor

temperature was lower than the indoor temperature in all the natural ventilation scenarios and at all times except between 14:00 and 16:00. However, in comparison to Scenario 1, where no natural ventilation is in effect, Scenarios 2 through 5 were all successful in lowering the indoor temperature anywhere between 0.83°C and 6.22°C. The temperature was fairly maintained inside the building despite the significant spike in outdoor temperature between 14:00 and 16:00. Cross ventilation (Scenario 3) and stack ventilation (Scenario 4) were the most efficient strategies in lowering the indoor temperature, with very similar values between 0:00 and 14:00. Cross ventilation was yet more impactful in lowering the temperature after 14:00 and exhibited the lowest indoor temperature 79% of this spring representative day. In scenario 5, when windows were opened at 21:00, the indoor temperature dropped instantly by over 3.50°C. Nevertheless, the indoor temperature remained higher than that in all other scenarios at all times, which proves its inefficacy in spring compared to other scenarios.

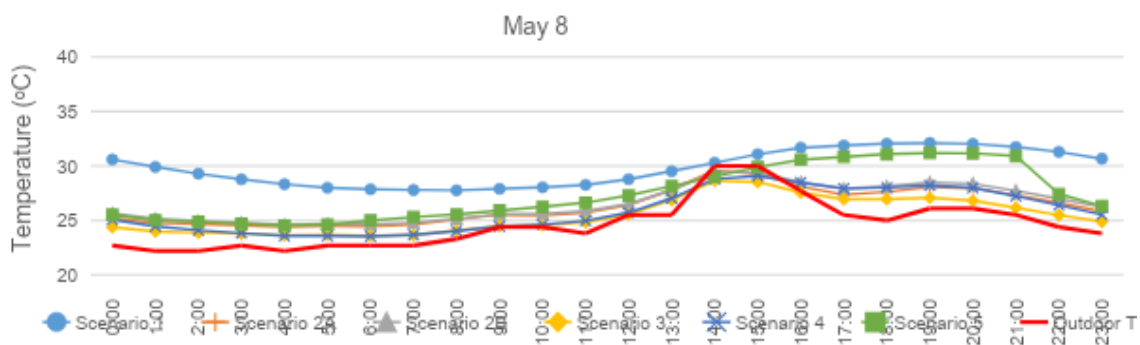


Figure 14. Comparison of the indoor temperatures in different scenarios and the outdoor temperatures on May 8, 2022 (spring representative day).

Figure 15 depicts an opposite trend on May 8, where relative humidity decreased with the surge in air temperature in Figure 14 since warm air can hold more moisture than cold air [52]. The outdoor relative humidity had a minimum value of 55% and reached a maximum of 100% at 3:00. Indoor relative humidity ranged between 49% and 64% in Scenario 1, between 55% and 83% in Scenario 2A, between 53% and 83% in Scenario 2B, between 58% and 87% in Scenario 3, between 52% and 88% in Scenario 4, and between 52% and 83% in Scenario 5. Particularly in scenario 1 (no

natural ventilation), the relative humidity values were the lowest among all scenarios 100% of the day. Among the natural ventilation strategies, night flush (Scenario 5) resulted in the lowest relative humidity value 58% of the day.

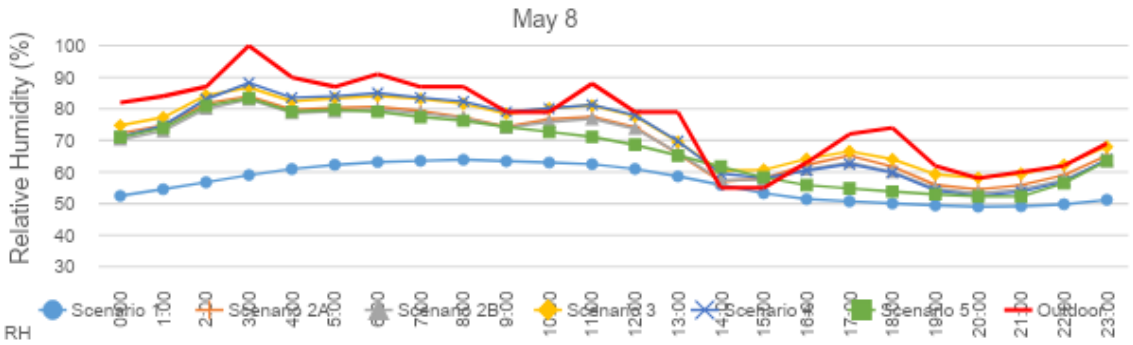


Figure 15. Comparison of the relative humidity in different scenarios and the outdoor relative humidity on May 8, 2022 (spring representative day).

During the summer representative day, Figure 16 shows that natural ventilation was inefficient in lowering indoor temperatures below the outdoor temperatures 100% of the day in Scenarios 1, 2, and 5 and 96% of the day in Scenarios 3 and 4. Compared to Scenario 1, natural ventilation caused the indoor temperature to decrease between 0.94°C and 7.79°C, a higher reduction than in spring. Similar to spring, Scenario 3 was the most efficient in lowering the indoor temperature, exhibiting the lowest temperature 100% of the day among all scenarios. Night flush (Scenario 5) was also the least effective natural ventilation strategy in summer.

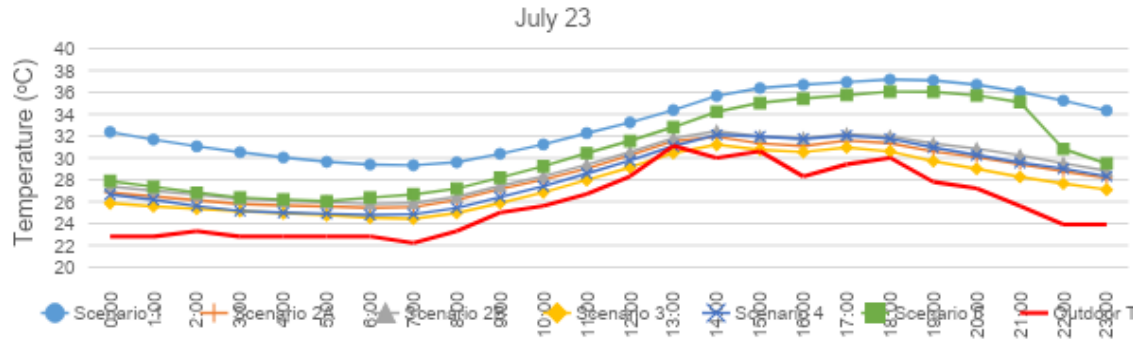


Figure 16. Comparison of the indoor temperatures in different scenarios and the outdoor temperatures on July 23, 2022 (summer representative day).

Figure 17 shows the same inverse relationship between relative humidity and temperature on the summer representative day as on the spring representative day.

The relative humidity ranged between 53% and 97% outdoor and between 40% and 66% in Scenario 1, between 52% and 83% in Scenario 2A, between 50% and 81% in Scenario 2B, between 54% and 87% in Scenario 3, between 50% and 85% in Scenario 4, and between 43% and 81% in Scenario 5. Similar to spring, Scenario 1 displayed the lowest relative humidity values 100% of the day, and night flush was the most efficient strategy in lowering relative humidity, with the lowest values 96% of the day, proving that this strategy is more efficient for this purpose in summer than in spring.

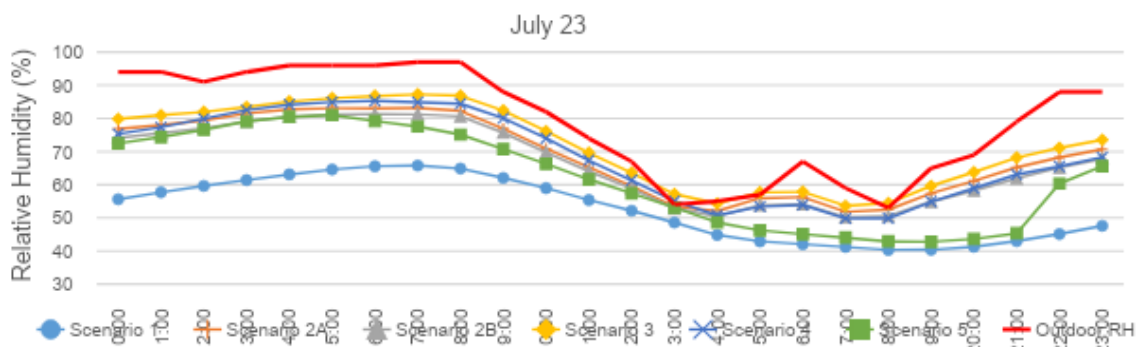


Figure 17. Comparison of the relative humidity in different scenarios and the outdoor relative humidity on July 23, 2022 (Summer representative day).

3.3. Thermal comfort analysis

Thermal comfort is “that condition of mind that expresses satisfaction with the thermal environment” [53]. It depends on several factors, such as temperature, relative humidity, airspeed, metabolic rate, clothing insulation, and mean radiant temperature. Thermal comfort ranges can be calculated using psychometric charts based on adaptive comfort standards. This study utilized the Center of the Built Environment (CBE) Thermal Comfort Tool, an online tool developed for thermal comfort calculations and visualizations [54] in compliance with ASHRAE55-2017 [55], ISO 7730:2005 [56] and EN16798-1:2019 [57] Standards to assess whether the selected natural ventilation strategies could deliver a thermally comfortable environment. To specify the thermal comfort zone for the case study, the selected variables were air temperature (°C) and relative humidity (%), the model chosen was the PMV method (PMV between -0.5 and +0.5, according to the standard), occupants were considered to have no local control

on airspeed, the value for airspeed was fixed at 0.1m/s for comparison purposes, metabolic rate was specified to 1.3 met according to ASHRAE 55, 2017, and the designated clothing level was 0.5 clo (typical summer indoor clothing).

Figure 18 displays the generated thermal comfort zone and the hourly environmental conditions resulting from the simulations of all scenarios and the hourly outdoor environmental conditions for the two representative days. Moreover, Table 5 summarizes the percentage of hours that fall within the thermal comfort zone on May 8 and July 23, and the percentage of comfortable hours each month of the study period [58]. Based on these results, all the natural ventilation scenarios successfully delivered thermally comfortable indoor conditions for parts of the day during the spring and summer, as opposed to no natural ventilation where occupant discomfort was in force 100% of the time. A more significant number of thermally comfortable hours was achieved on the spring representative day by all scenarios compared to the summer representative day, where higher temperatures were recorded. May featured the highest number of thermally comfortable hours indoor, followed by September, June, August, and finally July. Cross ventilation (Scenario 3) was the most successful strategy, and night flush cooling (Scenario 5) was the least effective approach. Stack ventilation (Scenario 4) and natural ventilation with openings at full capacity (Scenario 2A) similarly delivered thermal comfort. Decreasing the windows' opening size (Scenario 2B) reduced comfort hours. Finally, the environmental conditions were constantly better outdoor than indoor, regardless of the natural ventilation strategy applied.

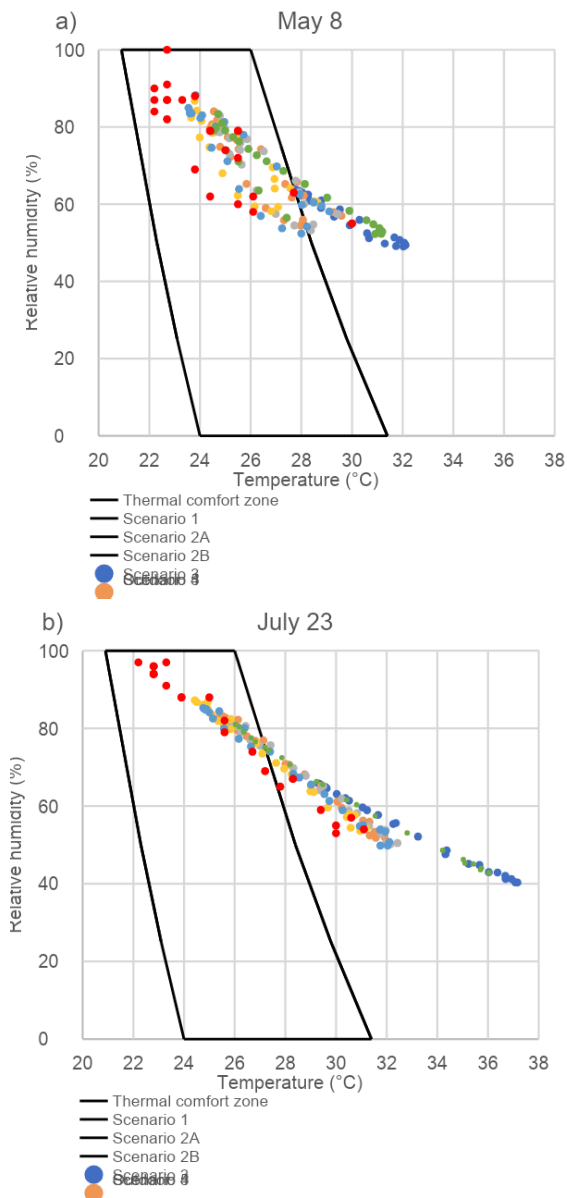


Figure 18. Thermal comfort analysis of the different scenarios and the outdoor environmental conditions on May 8 (a) and July 23 (b).

Table 5. Percentage of hours within the thermal comfort zone for the two representative days and monthly averages for the entire monitoring period

	May 8	July 23	May	June	July	August	September
Scenario 1	0%	0%	9%	0%	0%	0%	3%
Scenario 2A	83%	42%	77%	45%	36%	39%	65%
Scenario 2B	67%	33%	69%	32%	29%	31%	55%
Scenario 3	92%	50%	87%	49%	47%	51%	79%
Scenario 4	79%	42%	72%	48%	43%	46%	64%
Scenario 5	63%	29%	58%	28%	24%	27%	47%
Outdoor	96%	67%	89%	52%	58%	69%	81%

4. Conclusions

This study evaluated the efficiency of different natural ventilation strategies in cooling a historic residential building in a hot and humid climate zone. Historic structures possess distinctive characteristics and specific requirements that frequently impose limitations on acceptable interventions from both technological and architectural perspectives. Therefore, it is recommended to prioritize passive retrofit strategies and explore alternative cooling methods, such as natural ventilation, to uphold indoor thermal comfort while preserving the integrity of valuable historic materials, features, and values. The investigated strategies included natural ventilation with windows open at full and half capacity, cross ventilation, stack ventilation, and night ventilation. A scenario where no ventilation was in effect was also analyzed for comparison purposes. The methodology relied on using energy and Computational Fluid Dynamics (CFD) models calibrated using the onsite indoor environmental conditions, namely temperature and relative humidity, collected during the cooling season over five months. It is worth mentioning that this research methodology could be extended to the four seasons, however, as cooling is the most important challenge in ASHRAE Climate Zone 2A for human thermal comfort, this study focuses on the cooling period months. The analysis considered the building in its free-floating state, with no occupants or mechanical systems, to eliminate any factors that can influence natural ventilation patterns. The following results can be drawn from the current study:

- All investigated natural ventilation scenarios can reduce the cooling operation during spring and summer, particularly in spring, as they succeed in keeping air temperature and relative humidity values within the permitted ranges for occupant thermal comfort for parts of the day, as opposed to the case where no ventilation is in effect. However, mechanical cooling should be considered to provide a comfortable thermal environment for the remaining hours and preserve the heritage values embedded in the building, especially when relative humidity values are high.

- Natural ventilation with windows open, cross ventilation, and stack ventilation have a similar cooling pattern. During the spring season, they successfully lower temperatures visibly, especially in the exposed areas. Conversely, the temperatures are evenly distributed throughout the spaces in summer when outdoor temperatures are higher. Air velocity significantly impacts cooling and temperature distribution in the building. In both seasons, cross ventilation is the most efficient strategy for thermal comfort.
- Decreasing the opening size of the windows reduces air movement inside the building and lowers thermal comfort hours.
- Night ventilation reduces temperatures significantly once windows are open but fails to maintain lower temperatures throughout the day after the windows are closed, both in spring and summer. This strategy is the least effective in providing occupants' thermal comfort.
- Further research is required on implementing a holistic approach that considers thermal comfort and the preservation of the building and its historic materials and features. It is also recommended to consider the impact of other passive energy retrofit solutions and to evaluate the impact of natural ventilation as a strategy when coupled with these different retrofit approaches.

Finally, this methodology can enhance the understanding of the overall passive cooling approach in historic buildings, considering various financial and environmental perspectives. It aims to achieve a holistic and respectful building preservation of buildings, thereby creating a more resilient historic building stock capable of coping with potential future challenges posed by rising temperatures and humidity levels due to climate change. This investigative method is designed to be replicable, and its findings can be adapted to numerous historic buildings with similar construction typologies in hot and humid climates worldwide.

5. Acknowledgments

This research would not have been possible without the cooperation of the Power of Preservation (PoP) Foundation. The Building Performance Laboratory has supported this research. The authors would also like to acknowledge Assaad Akle, Panos Karaiskos, and Kylie Nixholm for their support in the study.

6. References

- [1] A. Martínez-Molina, I. Tort-Ausina, S. Cho, J.-L. Vivancos, Energy efficiency and thermal comfort in historic buildings: A review, *Renewable and Sustainable Energy Reviews*. 61 (2016) 70–85. <https://doi.org/10.1016/j.rser.2016.03.018>.
- [2] S. Michalski, Climate control priorities and solutions for collections in historic buildings, *Historic Preservation Forum*. 12 (1998) 8–14.
- [3] D. Camuffo, R. Van Grieken, H.J. Busse, G. Sturaro, Environmental monitoring in four European museums, *Atmos Environ*. 35 (2001) 127–140. [https://doi.org/10.1016/S1352-2310\(01\)00088-7](https://doi.org/10.1016/S1352-2310(01)00088-7).
- [4] P.O. Fanger, A.K. Melikov, H. Hanzawa, J. Ring, Air turbulence and sensation of draught, *Energy Build*. 12 (1988) 21–39. [https://doi.org/10.1016/0378-7788\(88\)90053-9](https://doi.org/10.1016/0378-7788(88)90053-9).
- [5] et al. Camuffo, Dario, Environmental monitoring in four European museums, *Atmos Environ*. 35 (2001) 127–140. [https://doi.org/10.1016/S1352-2310\(01\)00088-7](https://doi.org/10.1016/S1352-2310(01)00088-7).
- [6] National Trust for Historic Preservation, Energy Advice for Owners of Historic and Older Homes | US EPA ARCHIVE DOCUMENT, n.d. www.PreservationNation.org.
- [7] J.E. Hensley, A. Aguilar, Preservation Brief 3: Improving the Energy Efficiency in Historic Buildings, Washington DC, 2011. <http://www.nps.gov/history/hps/tps/briefs/brief03.htm> (accessed October 25, 2022).
- [8] E. Bay, A. Martinez-Molina, W.A. Dupont, Assessment of natural ventilation strategies in historical buildings in a hot and humid climate using energy and CFD simulations, *Journal of Building Engineering*. 51 (2022). <https://doi.org/10.1016/j.jobbe.2022.104287>.
- [9] E. Laurini, A. Taballione, M. Rotilio, P. De Berardinis, Analysis and exploitation of the stack ventilation in the historic context of high architectural, environmental and landscape value, in: *Energy Procedia*, Elsevier Ltd, 2017: pp. 268–280. <https://doi.org/10.1016/j.egypro.2017.09.386>.
- [10] M. Darmanis, M. Çakan, K.P. Moustris, K.A. Kavadias, K.S.P. Nikas, Utilisation of mass and night ventilation in decreasing cooling load demand, *Sustainability (Switzerland)*. 12 (2020). <https://doi.org/10.3390/SU12187826>.
- [11] W. Bordass, C. Bemrose, Heating your church, Council for the Care of Churches, Church House Publishing, London, 1996.
- [12] H.L. Schelle, Heating monumental churches-indoor climate and preservation of cultural heritage [Ph. D. thesis], Technical University of Eindhoven, The Netherlands. (2002).
- [13] Z. Spolnik, A. Worobiec, L. Samek, L. Bencs, K. Belikov, R. Van Grieken, Influence of different types of heating systems on particulate air pollutant deposition: The case of churches situated in a cold climate, *J Cult Herit*. 8 (2007) 7–12. <https://doi.org/https://doi.org/10.1016/j.culher.2006.09.003>.
- [14] D. Camuffo, E. Pagan, H. Schellen, D. Limpens-Neilen, R. Kozlowski, L. Bratasz, S. Rissanen, R. Van Grieken, Z. Spolnik, L. Bencs, Church heating and preservation of the cultural heritage: a practical guide to the pros and cons of various heating systems, *Electa Mon*. Milan: Electa Mondadori. (2007).

- [15] D. D' Agostino, P.M. Congedo, R. Cataldo, Ventilation Control using Computational Fluid-dynamics (CFD) Modelling for Cultural Buildings Conservation, *Procedia Chem.* 8 (2013) 83–91. <https://doi.org/https://doi.org/10.1016/j.proche.2013.03.012>.
- [16] Z. Huijbregts, R.P. Kramer, M.H.J. Martens, A.W.M. van Schijndel, H.L. Schellen, A proposed method to assess the damage risk of future climate change to museum objects in historic buildings, *Build Environ.* 55 (2012) 43–56. <https://doi.org/https://doi.org/10.1016/j.buildenv.2012.01.008>.
- [17] D. Camuffo, E. Pagan, S. Rissanen, Ł. Bratasz, R. Kozłowski, M. Camuffo, A. della Valle, An advanced church heating system favourable to artworks: A contribution to European standardisation, *J Cult Herit.* 11 (2010) 205–219. <https://doi.org/https://doi.org/10.1016/j.culher.2009.02.008>.
- [18] S. López-Aparicio, J. Smolík, L. Mašková, M. Součková, T. Grøntoft, L. Ondráčková, J. Stankiewicz, Relationship of indoor and outdoor air pollutants in a naturally ventilated historical building envelope, *Build Environ.* 46 (2011) 1460–1468. <https://doi.org/https://doi.org/10.1016/j.buildenv.2011.01.013>.
- [19] S.P. Corgnati, M. Perino, CFD application to optimise the ventilation strategy of Senate Room at Palazzo Madama in Turin (Italy), *J Cult Herit.* 14 (2013) 62–69. <https://doi.org/https://doi.org/10.1016/j.culher.2012.02.007>.
- [20] A. Martinez-Molina, M. Alamaniotis, Enhancing historic building performance with the use of fuzzy inference system to control the electric cooling system, *Sustainability (Switzerland)*. 12 (2020). <https://doi.org/10.3390/su12145848>.
- [21] A. Martinez-Molina, K. Williamson, W. Dupont, Thermal comfort assessment of stone historic religious buildings in a hot and humid climate during cooling season. A case study, *Energy Build.* 262 (2022) 111997. <https://doi.org/10.1016/j.enbuild.2022.111997>.
- [22] L. Bencs, Z. Spolnik, D. Limpens-Neilen, H.L. Schellen, B.A.H.G. Jütte, R. Van Grieken, Comparison of hot-air and low-radiant pew heating systems on the distribution and transport of gaseous air pollutants in the mountain church of Rocca Pietore from artwork conservation points of view, *J Cult Herit.* 8 (2007) 264–271. <https://doi.org/https://doi.org/10.1016/j.culher.2007.05.001>.
- [23] Ł. Bratasz, R. Kozłowski, D. Camuffo, E. Pagan, Impact of Indoor Heating on Painted Wood - Monitoring the Altarpiece in the Church of Santa Maria Maddalena in Rocca Pietore, Italy, *Studies in Conservation.* 52 (2007) 199–210. <https://doi.org/10.1179/sic.2007.52.3.199>.
- [24] A. Aflaki, N. Mahyuddin, Z. Al-Cheikh Mahmoud, M.R. Baharum, A review on natural ventilation applications through building façade components and ventilation openings in tropical climates, *Energy Build.* 101 (2015) 153–162. <https://doi.org/https://doi.org/10.1016/j.enbuild.2015.04.033>.
- [25] T. Hirano, S. Kato, S. Murakami, T. Ikaga, Y. Shiraishi, A study on a porous residential building model in hot and humid regions: Part 1 - The natural ventilation performance and the cooling load reduction effect of the building model, *Build Environ.* 41 (2006) 21–32. <https://doi.org/10.1016/j.buildenv.2005.01.018>.
- [26] Y. Chen, J. Gao, J. Yang, U. Berardi, G. Cui, An hour-ahead predictive control strategy for maximizing natural ventilation in passive buildings based on weather forecasting, *Appl Energy.* 333 (2023). <https://doi.org/10.1016/j.apenergy.2022.120613>.
- [27] E. Franzoni, B. Berk, M. Bassi, C. Marrone, An integrated approach to the monitoring of rising damp in historic brick masonry, *Constr Build Mater.* 370 (2023). <https://doi.org/10.1016/j.conbuildmat.2023.130631>.
- [28] K. Williamson, A. Martinez-Molina, W. Dupont, In Situ Assessment of HVAC System Impact in Façades of a UNESCO World Heritage Religious Building, *ANUARI d'Arquitectura i Societat.* (2021) 146–168. <https://doi.org/10.4995/anuari.2021.16331>.
- [29] P. V Nielsen, F. Allard, H.B. Awbi, L. Davidson, A. Schälin, Computational Fluid Dynamics in Ventilation Design REHVA Guidebook No 10, *International Journal of Ventilation.* 6 (2007) 291–294. <https://doi.org/10.1080/14733315.2007.11683784>.

- [30] M. Hajdukiewicz, M. Geron, M.M. Keane, Formal calibration methodology for CFD models of naturally ventilated indoor environments, *Build Environ.* 59 (2013) 290–302. <https://doi.org/https://doi.org/10.1016/j.buildenv.2012.08.027>.
- [31] C. Balocco, G. Grazzini, Plant refurbishment in historical buildings turned into museum, *Energy Build.* 39 (2007) 693–701. <https://doi.org/https://doi.org/10.1016/j.enbuild.2006.06.012>.
- [32] M. Abuku, H. Janssen, S. Roels, Impact of wind-driven rain on historic brick wall buildings in a moderately cold and humid climate: Numerical analyses of mould growth risk, indoor climate and energy consumption, *Energy Build.* 41 (2009) 101–110. <https://doi.org/https://doi.org/10.1016/j.enbuild.2008.07.011>.
- [33] C. Balocco, Daily natural heat convection in a historical hall, *J Cult Herit.* 8 (2007) 370–376. <https://doi.org/https://doi.org/10.1016/j.culher.2007.04.004>.
- [34] C. Balocco, G. Grazzini, Numerical simulation of ancient natural ventilation systems of historical buildings. A case study in Palermo, *J Cult Herit.* 10 (2009) 313–318. <https://doi.org/https://doi.org/10.1016/j.culher.2008.03.008>.
- [35] P.-C. Liu, H.-T. Lin, J.-H. Chou, Evaluation of buoyancy-driven ventilation in atrium buildings using computational fluid dynamics and reduced-scale air model, *Build Environ.* 44 (2009) 1970–1979. <https://doi.org/https://doi.org/10.1016/j.buildenv.2009.01.013>.
- [36] ASHRAE, ASHRAE, Museums, libraries and archives, *ASHRAE Handb. Heating, Vent. Air Cond. Appl.*, n.d.
- [37] P. Chassagne, E. Bou-Saïd, A. Ceccotti, J.-F. Jullien, M. Togni, The contribution of numerical simulation for the diagnosis of the conservation of art objects: Application to Antonio Santucci's armillary sphere of the 16th century, *J Cult Herit.* 8 (2007) 215–222. <https://doi.org/https://doi.org/10.1016/j.culher.2007.04.001>.
- [38] M. Kottek, J. Grieser, C. Beck, B. Rudolf, F. Rubel, World map of the Köppen-Geiger climate classification updated, *Meteorologische Zeitschrift.* 15 (2006) 259–263. <https://doi.org/10.1127/0941-2948/2006/0130>.
- [39] US Department of Commerce, National weather service, (2022). <https://www.weather.gov/wrh/Climate?wfo=ewx> (accessed September 10, 2022).
- [40] S. Huddleston, Long-neglected 1906 Kelso House in Monte Vista has beautiful new exterior — more work is needed, *San Antonio Express News.* (2022). <https://www.expressnews.com/news/local/article/1906-Kelso-House-in-Monte-Vista-rest-oration-work-17017952.php> (accessed July 5, 2022).
- [41] D.E. Everett, *San Antonio's Monte Vista: Architecture and Society in a Gilded Age, 1890-1930*, Maverick Pub. Co., San Antonio, TX, 1999.
- [42] G. Paliaga, L.J. Schoen, P.F. Alspach, E. a Arens, R.M. Aynsley, R. Bean, J. Eddy, T.B. Hartman, D. Int-hout, M. a Humphreys, E.E. Khalil, M.P.O. Rourke, P. Simmonds, J.L. Stoops, S.C. Turner, K.W. Cooper, W.F. Walter, D.S. Abramson, C.S. Barnaby, S.J. Emmerich, J.M. Ferguson, R.L. Hall, R.M. Harrold, *Thermal Environmental Conditions for Human Occupancy AHSRAE 55*, ASHRAE. (2013). <https://doi.org/ISSN 1041-2336>.
- [43] *Building Performance Modeling Handbook-2023v01*, (n.d.).
- [44] IES VE, (n.d.). <https://www.iesve.com/> (accessed May 31, 2023).
- [45] *CFD: MicroFlo User Guide IES VE 2015*, n.d.
- [46] E. Yohana, B. Yuniarto, R.P. Hunadika, S. Bahar, A.A. Muhammad, CFD Analysis of Temperature Distribution and Relative Humidity in Humidifying Sample House with Liquid Desiccant Concentration of 50% and Temperature of 10 °C, *Adv Sci Lett.* 23 (2017) 2243–2245. <https://doi.org/10.1166/asl.2017.8719>.
- [47] E. Bay, A. Martinez-Molina, W.A. Dupont, Assessment of natural ventilation strategies in historical buildings in a hot and humid climate using energy and CFD simulations, *Journal of Building Engineering.* 51 (2022). <https://doi.org/10.1016/j.job.2022.104287>.
- [48] C. Pérez-Vega, J.A. Ramírez-Arias, I.L. López-Cruz, R. Arteaga-Ramírez, R. Cervantes-Osornio, 3D computational fluid dynamics modeling of temperature and humidity in a humidified greenhouse, *Ingeniería Agrícola y Biosistemas.* 13 (2021) 17–31. <https://doi.org/10.5154/r.inagbi.2020.10.060>.

- [49] C. Lerma, J.G. Borràs, Á. Mas, M.E. Torner, J. Vercher, E. Gil, Evaluation of hygrothermal behaviour in heritage buildings through sensors, CFD modelling and IRT, *Sensors (Switzerland)*. 21 (2021) 1–19. <https://doi.org/10.3390/s21020566>.
- [50] ASHRAE Guideline 14, ASHRAE Guideline 14-2014: Measurement of Energy, Demand, and Water Savings, 2014.
- [51] B. Givoni, *Comfort, climate analysis and building design guidelines*, Energy Build. 18 (1992) 11–23. [https://doi.org/10.1016/0378-7788\(92\)90047-K](https://doi.org/10.1016/0378-7788(92)90047-K).
- [52] C.W. Callahan, A.M. Elansari, D.L. Fenton, Psychrometrics, in: *Postharvest Technology of Perishable Horticultural Commodities*, Elsevier, 2019: pp. 271–310. <https://doi.org/10.1016/B978-0-12-813276-0.00008-0>.
- [53] ANSI, ASHRAE. Standard 55 - thermal environmental conditions for human occupancy., 2017.
- [54] F. Tartarini, S. Schiavon, T. Cheung, T. Hoyt, CBE Thermal Comfort Tool : online tool for thermal comfort calculations and visualizations., *SoftwareX*. (2020).
- [55] ASHRAE Standing Standard Project Committee 55, ANSI/ASHRAE Standard 55, 2010. www.ashrae.org.
- [56] ISO, ISO 7730 - Ergonomics of the thermal environment - Analytical determination and interpretation of thermal comfort using calculation of the PMV and PPD indices and local thermal comfort criteria., 2005.
- [57] CEN, EN 16798-1 - Energy performance of buildings - Ventilation for buildings. Part 1: Indoor environmental input parameters for design and assessment of energy performance of buildings addressing indoor air quality, thermal environment, lighting and acoustics. , 2019.
- [58] M.K. Singh, R. Ooka, H.B. Rijal, S. Mahapatra, BUILDING SIMULATION BASED STUDY TO IMPROVE THERMAL PERFORMANCE OF A TRADITIONAL RESIDENTIAL HOUSE, in: *The Fifth International Conference on Human-Environment System*, Nagoya, 2016.